TU Delft

Delft University of Technology

Several Agent-Based and Cellular Automata Mathematical Frameworks for Modeling Pancreatic Cancer

Chen, Jiao; Vermolen, Fred J.

DOI
10.1007/978-3-030-55874-1_25

Publication date
2021

Document Version
Final published version

Published in
Numerical Mathematics and Advanced Applications, ENUMATH 2019 - European Conference

Citation (APA)
Chen, J., & Vermolen, F. J. (2021). Several Agent-Based and Cellular Automata Mathematical Frameworks for Modeling Pancreatic Cancer. In F. J. Vermolen, & C. Vuik (Eds.), *Numerical Mathematics and Advanced Applications, ENUMATH 2019 - European Conference* (pp. 265-274). (Lecture Notes in Computational Science and Engineering; Vol. 139). Springer. https://doi.org/10.1007/978-3-030-55874-1_25

Important note
To cite this publication, please use the final published version (if applicable).
Please check the document version above.

Copyright
Other than for strictly personal use, it is not permitted to download, forward or distribute the text or part of it, without the consent of the author(s) and/or copyright holder(s), unless the work is under an open content license such as Creative Commons.

Takedown policy
Please contact us and provide details if you believe this document breaches copyrights.
We will remove access to the work immediately and investigate your claim.

This work is downloaded from Delft University of Technology.
For technical reasons the number of authors shown on this cover page is limited to a maximum of 10.

Several Agent-Based and Cellular Automata Mathematical Frameworks for Modeling Pancreatic Cancer

Jiao Chen and Fred J. Vermolen

Abstract Mathematical modeling sheds light on cancer research. In addition to reducing animal-based experiments, mathematical modeling is able to provide predictions and prevalidate hypotheses quantitatively. In this work, two different agent-based frameworks regarding cancer modeling are summarised. In contrast, cell-based models focus on the behavior of every single cell and presents the interaction of cells on a small scale, whereas, cellular automata models are used to simulate the interaction of cells with their microenvironment on a large tissue scale.

1 Introduction

In agent-based modeling, a collection of autonomous decision-making entities (called agents) is utilized to model a system. Based on a set of rules, each agent makes the decision individually and executes various behaviors for the whole system [8]. Therefore, agent-based modeling represents a dynamic and interactive system, which has been applied in various fields like biomedical research [5], chemistry [10], market analysis [1], etc.

J. Chen (✉)
Delft Institute of Applied Mathematics, Delft University of Technology, Delft, The Netherlands

Department of Biomedical Engineering and Physics, Amsterdam UMC, Amsterdam, The Netherlands
e-mail: j.chen-6@tudelft.nl

F. J. Vermolen
Delft Institute of Applied Mathematics, Delft University of Technology, Delft, The Netherlands

Division of Mathematics and Statistics, Faculty of Sciences, Hasselt University, Diepenbeek, Belgium
e-mail: fred.vermolen@uhasselt.be

© Springer Nature Switzerland AG 2021

F. J. Vermolen, C. Vuik (eds.), *Numerical Mathematics and Advanced Applications ENUMATH 2019*, Lecture Notes in Computational Science and Engineering 139,
https://doi.org/10.1007/978-3-030-55874-1_25

Agent-based modeling is capable of simulating a broad spectrum of length-scales, which has been classified by Van Liedekerke et al. [11] into the following three types:

- **Lattice-based model**, where the model is developed based on regular lattice sites in a spatial computational domain. In biomedical modeling, cell bioprocesses are represented by transitions of each lattice state such that the model shows the evolution of a system by a discrete time-stepping mechanism or a continuous-time framework [9]. According to [11], the lattice-based model can be further classified into cellular automata models, lattice gas cellular and cellular potts models.
- **Off-lattice model**, which means the model is lattice-free and each agent is allowed to move in any direction rather than restricting agents to lattice sites. Some examples are center-based models, deformable cell models, and vertex model, etc. [11].
- **Hybrid discrete-continuum model**. To solve large multicellular systems, discrete agent-based models need large computational time since individual cells are concerned. The continuum model is able to solve PDEs for tissue dynamics or other complicated issues. Therefore, a hybrid discrete-continuum model is proposed to simulate multiscale models [11].

2 Agent-Based Models

Agent-based (or cell-based) models deal with biological cells as discrete entities in a computational domain. One of the advantages is the straightforward integration of cell-level processes like cell proliferation, cell death, cell mutation, etc. and the intracellular interactions. We develop a cell-based model with an application to pancreatic cancer therapy at early stages [5]. In this work, we consider three cell phenotypes, i.e. epithelial cells, cancer cells, T-lymphocytes, which are visualized as blue, red and green colored circles in Fig. 1, respectively. Figure 1 shows consecutive snapshots of the migration of T-lymphocytes in pancreatic cancer at an early stage. Since pancreatic cancer cells accumulate in rounded (three dimensional) clusters, we model the computational domain as a circular structure [5]. To visualize cell mutation, epithelial cells change color from blue to filled red. Moreover, other cell bioprocesses such as cell division and cell death are incorporated. Typically, in a competitive environment, cancer cells have a growth and proliferation (division) advantage over other healthy cells, therefore, the number of cancer cells in Fig. 1 accounts for the majority at time $= 150$ h.

In this model, the migration of epithelial and cancer cells is mechanotaxis updated by

$$\mathbf{r}_i^n = \mathbf{r}_i^{n-1} + \Delta t \alpha_i \hat{M}_i(\mathbf{r}^n) + \eta \Delta \mathbf{W}(t), \tag{1}$$

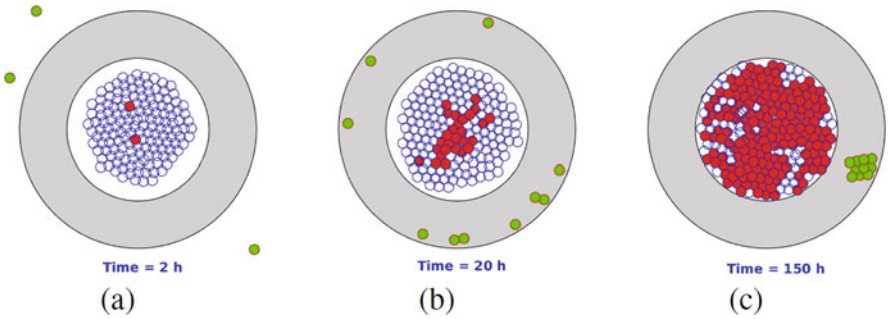

Fig. 1 Consecutive snapshots of cancer progression and T-lymphocytes migration when time = 2 h (**a**), time = 20 h (**b**) and time = 150 h (**c**), respectively. The blue, red and green color denote epithelial cells, cancer cells and T-lymphocytes

where $\mathbf{r}_i$ and α_i represents the position of cell i and its velocity parameter. The $\hat{M}_i(\mathbf{r})$ is the total mechanical signal comprising of traction force caused by strain energy density and a repulsive force. In addition, η denotes a constant and $\Delta\mathbf{W}(t)$ takes care of random walk (diffusion), which is a Wiener process. In contrast, the locomotion of T-lymphocytes is chemo-mechanotaxis, where T-lymphocytes are attracted by a type of chemokine secreted by cancer cells. The displacement of T-lymphocytes is described as

$$\mathbf{r}_j^n = \mathbf{r}_j^{n-1} + \beta\nabla c(t, \mathbf{r}_j^{n-1})\Delta t + \eta\Delta\mathbf{W} - M^{\mathrm{mc}}(\mathbf{r}_j^{n-1})\mathbf{z}_j^{n-1}\Delta t. \tag{2}$$

Here $c(t, \mathbf{r}_j^{n-1})$ denotes the concentration of chemokine secreted by cancer cells at time step $n-1$ and β is a constant. Whenever any two cells contact with each other, the repulsive force $M^{\mathrm{mc}}(\mathbf{r}_j)$ repels two cells with direction $\mathbf{z}_j$.

Next we consider a deformable cell model. The deformable cell model simulates the evolution of cell shape during the interaction with the microenvironment, see an example in [3]. In Fig. 2, some snapshots at consecutive times are plotted to show the deformation of a migrating cell and its nucleus denoted in red and green color, respectively. Furthermore, circles in grey color are regarded as two stiff obstacles and the cell penetrates the cavity by the attraction of two source points (blue asterisk). The migration of the cell and its nucleus is determined by chemotaxis, which can be expressed as

$$\mathbf{x}_i(t^{p+1}) = \mathbf{x}_i(t^p) + \Delta t\cdot(\beta\nabla c_i(t^{p+1}) + \alpha(\mathbf{x}_i^n(t^p) + \hat{\mathbf{x}}_i - \mathbf{x}_i(t^{p+1}))) + \eta\Delta\mathbf{W}, \tag{3}$$

and

$$\mathbf{x}_i^n(t^{p+1}) = \mathbf{x}_i^n(t^p) + \Delta t\cdot(-\alpha(\mathbf{x}_i^n(t^p) + \hat{\mathbf{x}}_i - \mathbf{x}_i(t^{p+1})) + \alpha^n(\mathbf{x}_c(t^p) + \hat{\mathbf{x}}_i^n - \mathbf{x}_i^n(t^{p+1}))) + \eta\Delta\mathbf{W}. \tag{4}$$

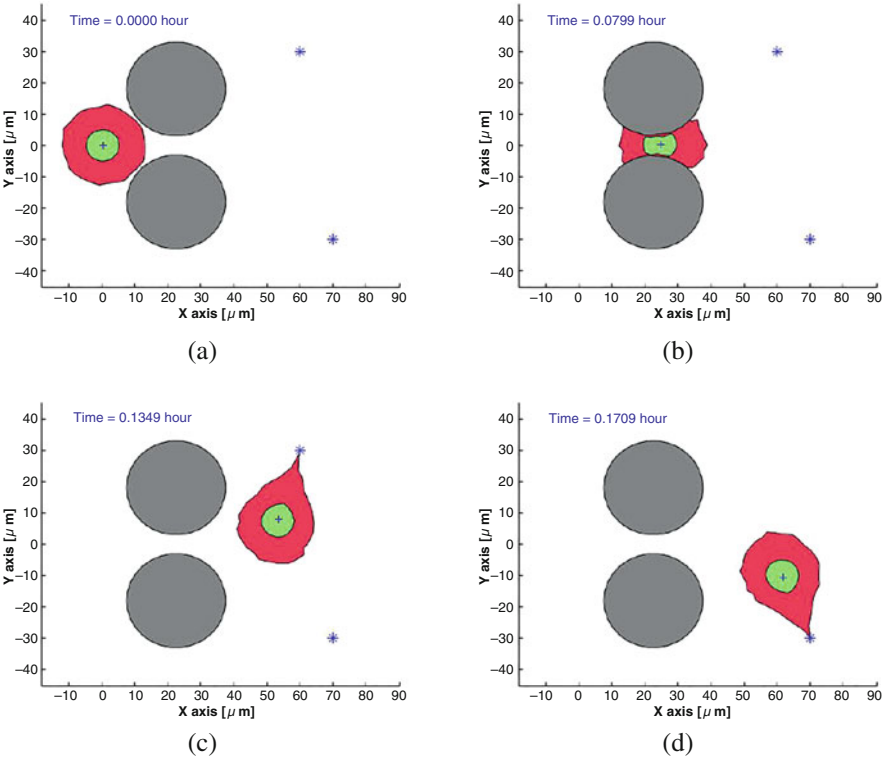

Fig. 2 Consecutive snapshots of the deformation of one migrating cell and its nucleus when time = 0 h, time = 0.0799 h, time = 0.1349 h and time = 0.1709 h, in red and green color, respectively. Two stiff obstacles are visualized in grey circles and source points are denoted by blue asterisks

Note that $\mathbf{x}_i$ and $\mathbf{x}_i^n$ denote the location of a node i on the cell membrane and nucleus surface, respectively. The second term in Eqs. (3) and (4) represents the interaction between the nucleus surface and cell membrane. Analogously, we model random walk by using a Wiener process $\Delta\mathbf{W}$, where η is a constant.

Cells are subject to large deformation during migration to adapt to the environment. This cell-based model can be applied to the deformation of an immune cell with the attraction of a pathogen source. In addition, it also can be used to describe the deformation of a cancer cell during the migration to the oxygen source as part of the metastasis process.

3 The Cellular Automata Model

The cellular automata model is a lattice-based method, which has been used in various fields. Specifically, a computational domain is divided into lattice sites,

where each lattice site can be occupied by one cell or multiple cells. Each lattice site can be in a discrete state and is able to 'jump' from one state into another state. Moreover, one single cell is able to share a few lattice sites in some cases. We develop a three-dimensional model to simulate the cancer progression and recession under virotherapy [2], in which one lattice point is occupied by multiple cells. As a result, Fig. 3 shows cancer progression at early stages in a $15\times15\times15$ mm^3 domain. To mimic cell mutation, epithelial cells (in blue color) are allowed to turn into cancer cells (in red color). As mentioned earlier, cancer cells have more growth and division rates than normal cells in a competitive environment with limited space and nutrition. The number of cancer cells increases significantly and thereby cancer progresses to a large volumetric fraction in the simulations.

In the model, any lattice site has three discrete states, i.e. unoccupied (or dead cell) state, epithelial cell state, cancer cell state. Under certain conditions, a lattice

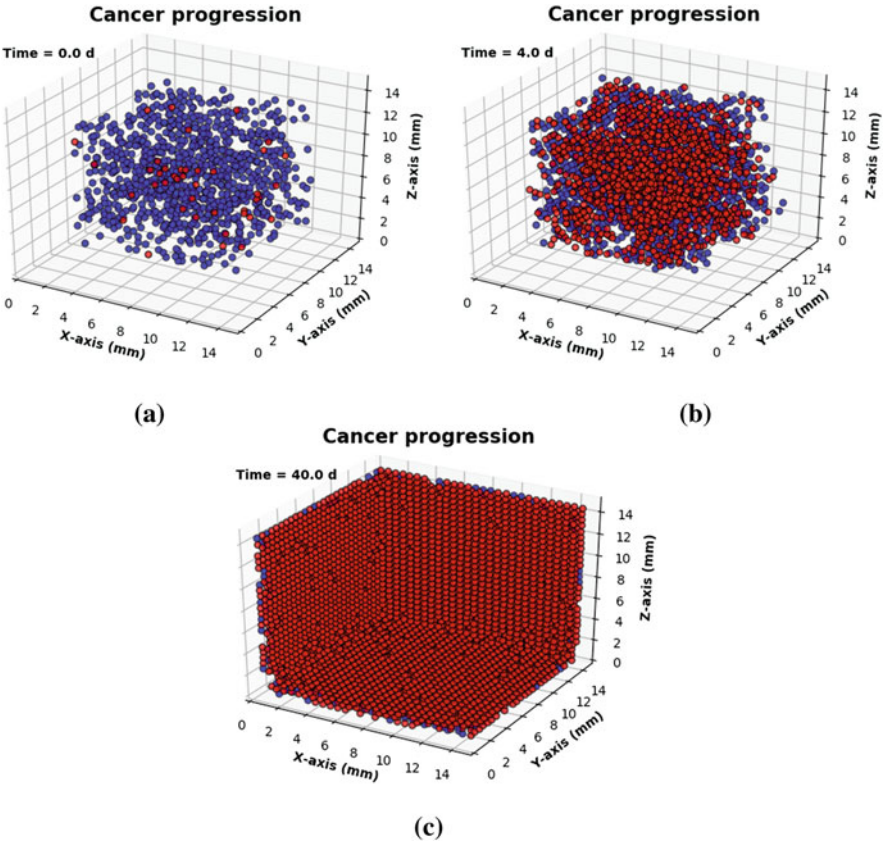

Fig. 3 Consecutive snapshots of cancer progression when time = 0 days, time = 4 days and time = 40 days, respectively, in cellular automata model. The blue and red color represent epithelial cells and cancer cells. The computational domain is $15\times15\times15$ mm^3

point, i, can change state and the transition probability P within a time interval (t_0, $t_0 + \Delta t$) is defined as

$$P = \int_{t_0}^{t_0+\Delta t} f(\lambda_i, t)\mathrm{d}t \simeq 1 - \exp(-\lambda_i \Delta t). \tag{5}$$

where $f(\lambda_i, t)$ is an exponential distribution and λ_i denotes the probability rate at grid node i per unit of time of state transition. Note that the probability rate for the change of state depends on the two states between which the grid node undergoes the change. Regarding our model, one of the merits is the flexibility of the input parameters. With proper input variables, our numerical results can reproduce experimental results very well, see Fig. 4 [2], where curves show cancer growth during 50 days. Taking the animal-based experimental results from [6], cancer grows under gemcitabine intervention compared with a control experiment showing in the blue line and black line in Fig. 4. In comparison, modeled results indicated by the red lines are able to predict the cancer progression well according to experimental curves.

Subsequently, this cellular automata model is extended to oncolytic virotherapy in pancreatic cancer at early stages [2]. We assume that a three-dimensional domain is fully colonized by cancer cells and at a certain time a dose of viruses is given

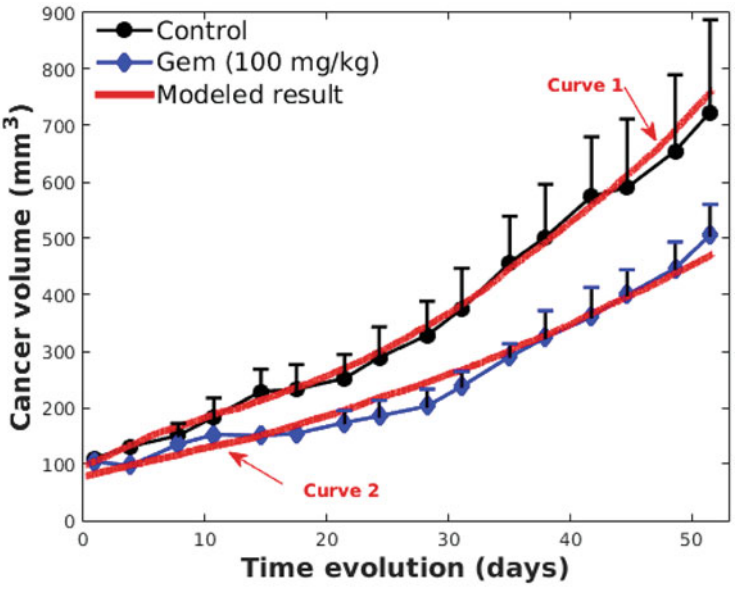

Fig. 4 Cancer growth with the respect of time in days [2]. The red curves show the numerical results from the cellular automata model, whereas the black and blue lines represent the cancer growth without gemcitabine and with gemcitabine, respectively. The experimental results are taken from the work [6]

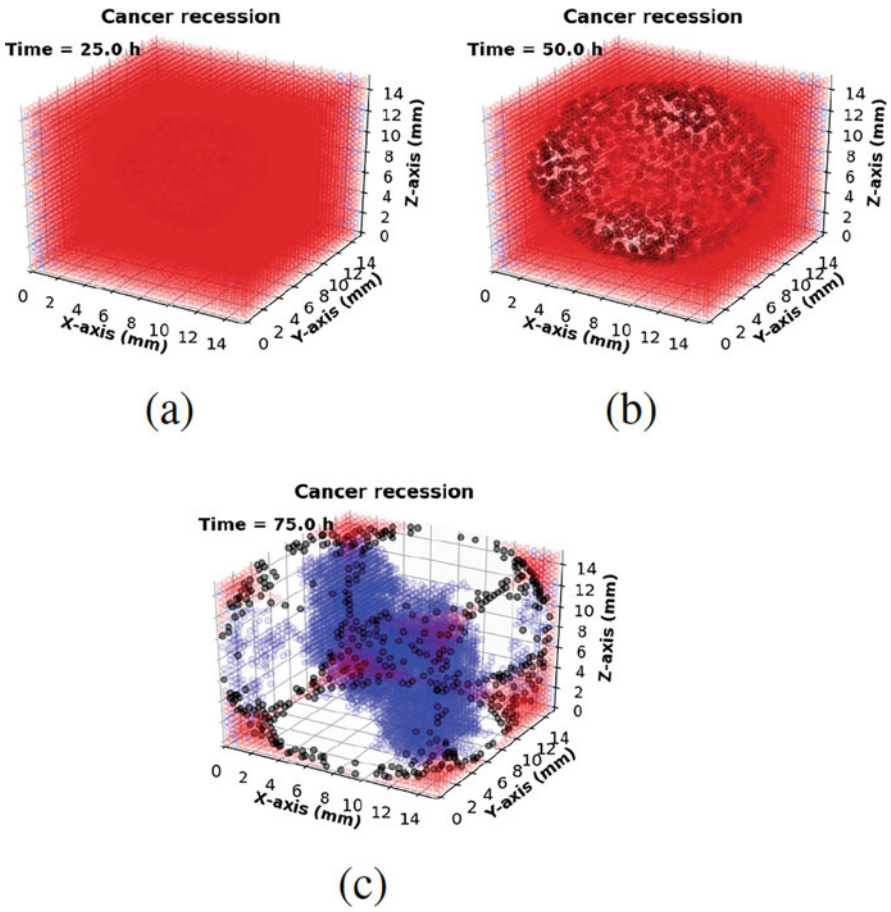

Fig. 5 Consecutive snapshots of cancer recession when time = 25 h, time = 50 h and time = 75 h, respectively, in cellular automata model with an application to virotherapy in pancreatic cancer. In the computational domain $15\times15\times15$ mm^3, the epithelial cells, cancer cells, infected cells are denoted in blue, red and black color, respectively. In addition, the lattice sites in white color represent the dead cells or unoccupied states

intratumorally by injection (see Fig. 5). Figure 5 shows cancer recession under virotherapy, where cancer cells, epithelial cells, infected cells are visualized in red, blue and black color, respectively. Once cancer cells die due to viral replication, the lattice points will transform from the cancer state to the unoccupied state, which is indicated in white color. Since the viruses are injected in the center of the domain, viruses diffuse and infect cancer cells from the central lattice points with the evolution of time (see Fig. 5b). The model of viral diffusion is defined as

$$\begin{cases} \frac{\partial c(\mathbf{r})}{\partial t} = D\Delta c(\mathbf{r}) + \gamma(t)\delta(\mathbf{x} - \mathbf{x}_p) + \beta c(\mathbf{r})(1 - \frac{c(\mathbf{r})}{N_v}) \\ D\frac{\partial c(\mathbf{r})}{\partial n} + Tc(\mathbf{r}) = 0, \quad \text{on } \partial\Gamma \end{cases}, \tag{6}$$

where c(**r**) is the viral concentration at any lattice point and D denotes the viral diffusivity. The Dirac delta function $\delta(\mathbf{x})$ mimics the viral source with a time-related secretion rate $\gamma(t)$ at position $\mathbf{x}_p$. Note that $\beta c(\mathbf{r})(1 - \frac{c(\mathbf{r})}{N_v})$ is a reaction term to simulate the viral replication, which only takes place in the grid nodes that are in the cancer state. Here β denotes the proliferation rate of virus and N_v represents a burst size of viruses. On the boundary Γ, viruses are able to disperse to the neighbor tissue or organs with a mass transfer rate coefficient T. As more and more cancer cells are eliminated by viruses, there is a 'wound' region, characterized by cells in the 'unoccupied state' appearing in the tissue as a result. However, healthy cells migrate to this wound from neighbor tissue or organs and hence fill in this gap by proliferation. In other words, this model could also be used for simulating wound healing.

4 Uncertainty Quantification

Using the cell deformation model, see Eqs. (3)–(4) and Fig. 2, we quantify the influence of uncertainty in the input data on the time of metastasis, which is modeled by the time at which a cancer cell exists a blood vessel. In the modeling set-up, cancer cells transmigrate through the walls of a blood vessel and subsequently they are transported by the bloodstream to enter at a different part of the body where they can colonize by forming new tumors. The set-up deviates from Fig. 2, more details can be found in [4]. The uncertainty quantification is performed by Monte Carlo simulations, see [7], in which the input parameters, here the cell size and the size of the aperture of the blood vessel are sampled from statistical distributions. The results indicate a significant positive correlation (sample correlation coefficient $r = 0.79$) between the metastasis time and the cell size. Hence the larger the cancer cell, the more time it takes to metastasize since transmigration through a blood vessel is more difficult for larger cells. Furthermore, the Monte Carlo simulations hint at a weaker negative correlation ($r = -0.17$) between the metastasis time and the size of the aperture of the vessel. This confirms the intuition that a permeable vessel facilitates the transmigration of the cell, and hence enhances metastasis (Fig. 6).

Moreover, the Monte Carlo method is further used to predict the likelihood of successful cancer treatment in our other works [2, 5]. The corresponding results are hopeful to aid experiment design and prevalidation before clinical trials.

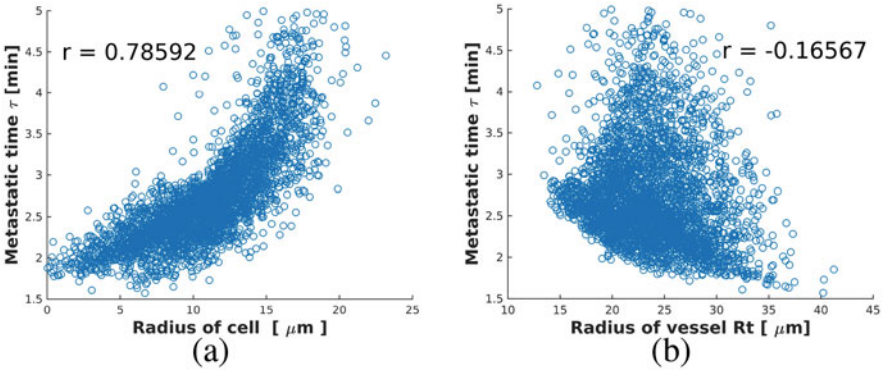

Fig. 6 Scatter plots of Monte Carlo simulations [4]. (**a**) Correlation between cell size and cell metastatic time with coefficient r = 0.78592; (**b**) correlation between vessel size and cell metastatic time with coefficient r = −0.16567

5 Discussion and Conclusions

Regarding cancer modeling, we develop different agent-based frameworks, namely the cell-based model and cellular automata model, which are compared in this paper. The cell-based model, where each individual cell is considered, is beneficial for modeling at small scales. The morphology of the cells can be fixed as in the model applied in pancreatic cancer at early stages [5]. Furthermore, one can zoom into the process of cell migration where one models morphological changes of each cell, such as in the simulation framework with an application to cancer metastasis [3]. Furthermore, the intercellular biomechanics and interactions between cells and their microenvironment are incorporated. However, with an increase in the number of cells, the cell-based model will be time-consuming, and therefore cellular automata model could be a computationally 'cheap' alternative. Besides the cellular automata model, a continuum model for the viral spread is taken into account by using the reaction-diffusion equation [2]. As we expected, the numerical results show consistency with the results from the experiments in the literature.

Computational modeling has played and will continue to play a pivotal role in cancer research and treatment. The computational framework will possess aspects from both complicated physics-based approaches as well as from 'simple' tractable phenomenological modeling approaches.

References

1. A Charania and D DePasquale. Economic modeling of future space markets. In *NewSpace 2006 Conference, Las Vegas, Nevada*, 2006.
2. Jiao Chen, Daphne Weihs, and Fred J Vermolen. A cellular automata model of oncolytic virotherapy in pancreatic cancer. *Bulletin of Mathematical Biology*, 82(8):1–25, 2020.

3. Jiao Chen, Daphne Weihs, Marcel Van Dijk, and Fred J Vermolen. A phenomenological model for cell and nucleus deformation during cancer metastasis. *Biomechanics and modeling in mechanobiology*, 17(5):1429–1450, 2018a.
4. Jiao Chen, Daphne Weihs, and Fred J Vermolen. Monte Carlo uncertainty quantification in modelling cell deformation during cancer metastasis. *Proceedings of the CMBBE2018*, 2018b.
5. Jiao Chen, Daphne Weihs, and Fred J Vermolen. Computational modeling of therapy on pancreatic cancer in its early stages. *Biomechanics and modeling in mechanobiology*, pages 1–18, 2019.
6. David E Durrant, Anindita Das, Samya Dyer, Seyedmehrad Tavallai, Paul Dent, and Rakesh C Kukreja. Targeted inhibition of phosphoinositide 3-kinase/mammalian target of rapamycin sensitizes pancreatic cancer cells to doxorubicin without exacerbating cardiac toxicity. *Molecular pharmacology*, 88(3):512–523, 2015.
7. John Hammersley. *Monte Carlo methods*. Springer Science & Business Media, 2013.
8. Charles M Macal and Michael J North. Tutorial on agent-based modeling and simulation. In *Proceedings of the Winter Simulation Conference, 2005.*, pages 14–pp. IEEE, 2005.
9. Michael J Plank and Matthew J Simpson. Models of collective cell behaviour with crowding effects: comparing lattice-based and lattice-free approaches. *Journal of the Royal Society Interface*, 9(76):2983–2996, 2012.
10. Alessandro Troisi, Vance Wong, and Mark A Ratner. An agent-based approach for modeling molecular self-organization. *Proceedings of the National Academy of Sciences*, 102(2):255–260, 2005.
11. Paul Van Liedekerke, MM Palm, N Jagiella, and Dirk Drasdo. Simulating tissue mechanics with agent-based models: concepts, perspectives and some novel results. *Computational particle mechanics*, 2(4):401–444, 2015.